Available online at www.sciencedirect.com
SCIENCE DIRECT
Catalysis Today 111 (2006) 68–73
CATALYSIS TODAY
www.elsevier.com/locate/cattod

Atomic-scale studies of metallic nanocluster catalysts by in situ high-resolution transmission electron microscopy

Stig Helveg *, Poul L. Hansen

Haldor Topsøe A/S, Nymøllevej 55, DK-2800 Kgs. Lyngby, Denmark

Available online 28 November 2005

Abstract

Recently, we studied the interaction of supported metal nanocluster catalysts with reactive gases at elevated temperatures by means of in situ high resolution transmission electron microscopy (HRTEM). This paper will briefly review this work to illustrate the in situ HRTEM capability for studies of the surface structures and the dynamics of supported metal nanoclusters at the atomic scale and to discuss the possibilities of including such insight into the description of their catalytic properties.

Keywords: High resolution transmission electron microscopy; Nanocrystals; Catalysts; In situ HRTEM; ETEM; Nanofibers; Dynamics

1. Introduction

With the recent advance of transmission electron microscopy techniques, scientists now have tools for directly probing the geometric, and in some cases also the compositional and electronic, structures of nanostructured catalysts with a real-space resolution down to the atomic level, e.g., Refs. [1,2]. This has opened up for new possibilities for obtaining structural information, for example, about the size, shape and detailed surface structure of nanomaterials, which is essential for the understanding of their catalytic properties, see, e.g., Refs. [3,4]. Up to now, electron microscopy studies of catalysts at the atomic-scale have mainly been performed ex situ after various gas treatments where the catalysts are removed from the reaction environments and studied under the high vacuum conditions residing in the electron microscope, see, e.g., Refs. [5–8]. Although this approach undoubtedly has a significant impact on catalysis research, the catalysts may respond dynamically to changes in the surrounding gas environment, and so, caution must be exercised to ensure that the observed structural details are representative of the catalyst in its working state.

On the other hand, the application of TEM to in situ studies of catalysts during exposure to reactive gas environments and elevated temperatures is fairly scarce. Such studies are by no means trivial due to the extremely small mean-free path of electrons in dense media (gases and solids), and significant instrumental modifications are needed in order to confine a high-pressure gas environment around the specimen area without affecting the microscope performance [9–13]. In the 1970s, Baker and co-workers performed the pioneering applications of in situ transmission electron microscopy for studies of nanocluster catalysts using an instrument with a resolution of about 3 nm [9,10]. In the 1990s, Boyes and Gai made a significant instrumental advancement and demonstrated an image resolution of 0.23 nm, allowing HRTEM imaging of the largest lattice spacing in noble metal catalysts [11]. However, in order to get detailed structural information about industrially important catalytic metals, such as Fe, Ni and Cu, a resolution of at least 0.18 nm is required. A collaboration between Haldor Topsøe A/S and the FEI Company realized this goal and, after further modifications, established an in situ HRTEM facility capable of providing the first images with a resolution of 0.14 nm during exposure of the sample to reactive gases and elevated temperatures [14].

In this paper, we outline recent examples from our research that exploit this in situ HRTEM capability for the study of supported metal nanocluster catalysts. The examples demonstrate how atomic-scale information can be obtained about, on one hand, the exposed metal surface sites and metal–support interfaces, and on the other hand, surface dynamic processes induced by changes in the gas environment. The reader is referred to the original papers [14–16] for an in-depth discussion of the

* Corresponding author.
E-mail address: sth@topsoe.dk (S. Helveg).

0920-5861/$ – see front matter
doi:10.1016/j.cattod.2005.10.019

results and to reviews, such as Refs. [10–12,17], for a detailed description of in situ HRTEM (which is also referred to as environmental TEM (ETEM) [11,12]).

2. Dynamic shape changes in supported copper nanocrystals

One of the simplifying assumptions in the description of catalytic reactions has often been to consider the catalyst surfaces as static, thus providing a fixed ensemble of active sites. However, there is no guarantee that the catalyst nanostructures remain stable during application. In situ studies have shown that metallic nanoclusters may undergo structural transformations in response to changes in the reaction conditions and that the transformations can have a significant impact on the catalytic performance [18–20]. In most cases, in situ spectroscopic methods have been used for investigations of the nanoclusters under catalytic relevant conditions [21–23], whereas complementary real-space insight, at the atomic level, into the dynamic structure and morphology of the metal nanoclusters under similar conditions has not previously been available.

In the following we will demonstrate that in situ HRTEM can provide unprecedented new insight about gas-induced nanocluster dynamics by focusing on a Cu/ZnO-based catalyst [14,15]. This catalyst system represents the industrial methanol synthesis catalyst and has become a prototype system for studying complex gas-induced structural dynamics [19,20,24–26]. Fig. 1 shows in situ HRTEM images of Cu nanocrystals supported on ZnO. The Cu nanocrystals are produced in situ by reduction of the CuO/ZnO precursor in hydrogen at 280 °C [14,15]. The lattice fringes in the nanoclusters, as well as the electron energy loss spectroscopy (EELS) data, confirm the presence of metallic Cu nanocrystals with diameters of 3–6 nm (Fig. 1A). To study the response of the Cu nanocrystals to variations in the gas composition, the catalyst was exposed to more oxidizing conditions by adding H_2O vapor to the hydrogen gas or to more reducing conditions by adding CO to the hydrogen gas. Upon each change in gas atmosphere, the Cu nanocrystals changed shape. Images were recorded during these changes. Fig. 1 shows HRTEM images representing the equilibrium shapes obtained by the Cu nanocrystals on the ZnO support.

Inspection of the in situ HRTEM images in Fig. 1 provides direct insight into the gas-induced shape changes and helps to elucidate the driving forces for the transformations: addition of H_2O is seen to result in Cu particles with a more spherical shape, i.e. the Cu nanocrystals are terminated by a higher fraction of (1 1 0) and (1 0 0) facets, relative to the more closed-packed (1 1 1) facet, than in pure hydrogen. Hence, the more open (1 1 0) and (1 0 0) facets tend to stabilize with respect to the (1 1 1) facet. At the interface, the contact area between Cu and ZnO does not change significantly. This points to the fact that water adsorption on the different exposed Cu facets is the main driving force for the gas-induced surface reconstructions and the resulting reshaping of the Cu nanocrystals. On the other hand, addition of the more reducing gas, carbon monoxide, to the hydrogen gas results in more marked changes. The Cu nanocrystals are found to transform into disc-like structures caused by an increased wetting of the ZnO support. On average, the interfacial area increases by about 50% indicating a large decrease in the interface energy. Previously, it was suggested that CO mainly affects the ZnO surface energy whereas the Cu surface energies are not perturbed [19,20,24]. This is probably a good approximation because the coverage of hydrogen and carbon monoxide on the Cu surfaces is fairly low under the conditions used here [19,24]. It was proposed that a change in the oxidation potential of the gas phase may change the oxygen content in the ZnO surface and thereby the interface energy [19,20,24]. Under more reducing conditions, the oxygen

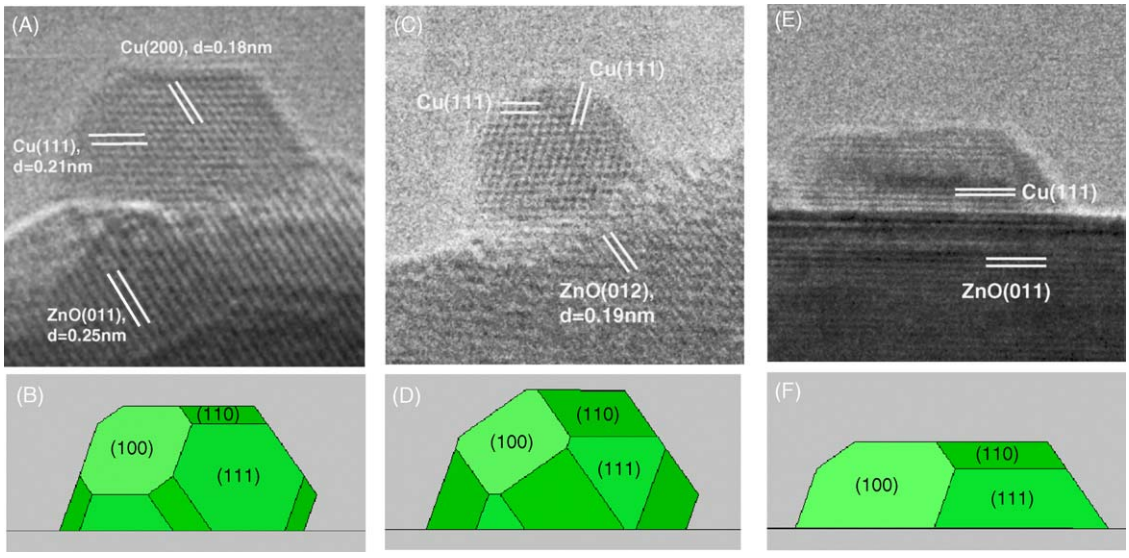

Fig. 1. In situ HRTEM images (A, C and E) of a Cu/ZnO catalyst in various gas environments together with the corresponding Wulff constructions (B, D and F) of the Cu nanocrystals. (A) The image was recorded at a pressure of 1.5 mbar of H_2 at 220 °C. The electron beam is parallel to the [0 1 1] zone-axis of copper. (C) The image was obtained with the Cu nanocrystal exposed to a gas mixture of H_2 and H_2O, H_2:H_2O = 3:1 at a total pressure of 1.5 mbar at 220 °C. (E) The image was obtained with the Cu nanocrystal exposed to a gas mixture of H_2 (95%) and CO (5%) at a total pressure of 5 mbar at 220 °C. Adapted from Ref. [14].

content in the ZnO surface will be low resulting in a decrease of the Cu/ZnO_x interface energy due to a partial (full) reduction of the ZnO surface layer, and vice versa. A combination of the in situ HRTEM results with in situ EELS measurements partly supports this interpretation [15]. As the reduction potential of the gas phase is increased, changes are observed in the energy-loss near-edge structure of the Cu L_3 ionization edge which can be attributed to a Cu–Zn alloy formation at the Cu–Zn interface or at the Cu surface, in accordance with previous suggestions [19,20,24,25].

The in situ electron microscopy results for the Cu/ZnO catalyst are not only in accordance with previous in situ extended X-ray absorption fine structure (EXAFS) data concerning the dynamic morphology changes [19,20], they also provide important new insight. On the basis of the lattice-resolved images, the exposed facets of the projected Cu nanocrystal and the epitaxial relationship between Cu and ZnO can be identified. The majority of the Cu nanocrystals appears to be in contact with the ZnO support with their (1 1 1) facet, as also observed for Cu particles prepared by vapor deposition under ultra-high vacuum conditions onto various atomically clean ZnO surfaces [27]. For the Cu/ZnO catalyst, the ZnO termination at the interface varies from particle to particle indicating a weak interaction and no strong preference for Cu to bind to specific ZnO facets. Furthermore, the lattice-resolved images allow Wulff constructions to be performed for the Cu nanocrystals, as shown in Fig. 1, and a quantitative determination of the relative metal surface free energies and the interface free energy in the different gas environments to be obtained [14]. Previously such quantitative information about supported nanoclusters could only be obtained from ex situ microscopy observations [28] or scanning tunneling microscopy studies under ultra-high vacuum conditions [29,30]. The ability to determine surface free energies in situ represents important perspectives. The surface and interface energies allow a reconstruction of the full three-dimensional shape of the supported Cu nanocrystals which in turn may provide important information about the concentration of the different types of surface sites (low-indexed planes, corners, steps, etc.) under the various gas conditions (Fig. 2). This allows the nanocluster morphology and information about site-specific reactivity to be incorporated more directly into the microkinetic description of a catalytic reaction with the approach discussed earlier for, e.g., the methanol synthesis reaction [24]. Previous microkinetic descriptions of catalysis had to rely on assumptions regarding the nature of the exposed surfaces and interfaces, as well as their dependence on the gas composition.

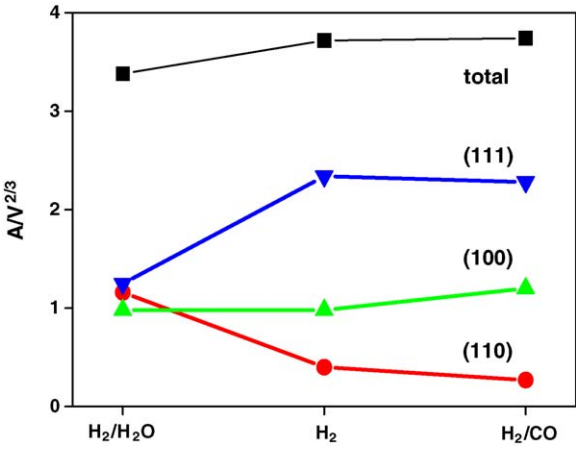

Fig. 2. The dimensionless surface area $A/V^{2/3}$ of the different low-index Cu facets, as well as the total surface area, vs. the gas environments in Fig. 1. The surface area distributions are determined from the Wulff constructions for a Cu nanocrystal, assuming that the nanocrystal is attached to the support on one of the (1 1 1) planes and that its shape is determined by the surface and interface free energies reported in Ref. [14].

3. Carbon nanofiber growth catalyzed by nickel nanocrystals

In situ TEM can also be applied in a dynamic mode, where the gas-induced restructuring of the nanoclusters is directly visualized by recording time-lapse image series and replaying these in the form of a movie. This has led to unprecedented new insight into the mechanistic details of gas-induced restructuring processes, such as reshaping, phase transformations, sintering and vapor deposition growth processes, e.g., Refs. [31–34]. In fact, Baker et al. used in their pioneering studies in situ TEM to monitor carbon nanofiber growth by catalytic acetylene decomposition over nickel nanoclusters [35,36]. The catalyzed growth of carbon nanofibers has achieved much attention because the process, on one hand, is important to inhibit in order to prevent breakdown of industrial steam reforming catalysts [37–39], and on the other hand, offers new synthesis routes for nanofibers with predefined structures and functionalities [40,41]. However, despite numerous studies, many fundamental questions related to the structure and dynamics of the catalyst surfaces during growth have not been possible to resolve due to the lack of atomic-resolved real-space insight.

From our results of this classic example of nickel-catalyzed formation of carbon nanofibers [16], we will demonstrate that in situ HRTEM has a potential for visualizing the dynamics of surface reactions on metal nanocluster at the atomic-scale. In the in situ HRTEM experiments, carbon nanofibers are formed by methane decomposition over oxide-supported Ni nanocrystals with diameters ranging from about 5 to 20 nm. The HRTEM images reveal that the Ni nanoclusters, located at the front end of the nanofibers, undergo a reaction-induced reshaping and that the nanocluster shape acts as a template for the alignment of graphene layers into multi-walled carbon nanofiber structures (Fig. 3). The smaller Ni nanoclusters tend to obtain highly elongated shapes, and tubular nanofibers form with the graphene layers aligned along the fiber axis. The larger Ni clusters tend to become pear-shaped, and whisker-like graphitic nanofibers emerge having the graphene layers inclined with respect to the fiber axis.

In situ HRTEM movies were recorded to monitor the dynamics in the growth process [42]. Fig. 4 shows an image series, which is extracted from such a movie and demonstrates the main findings [16]. It is observed that the initial compact

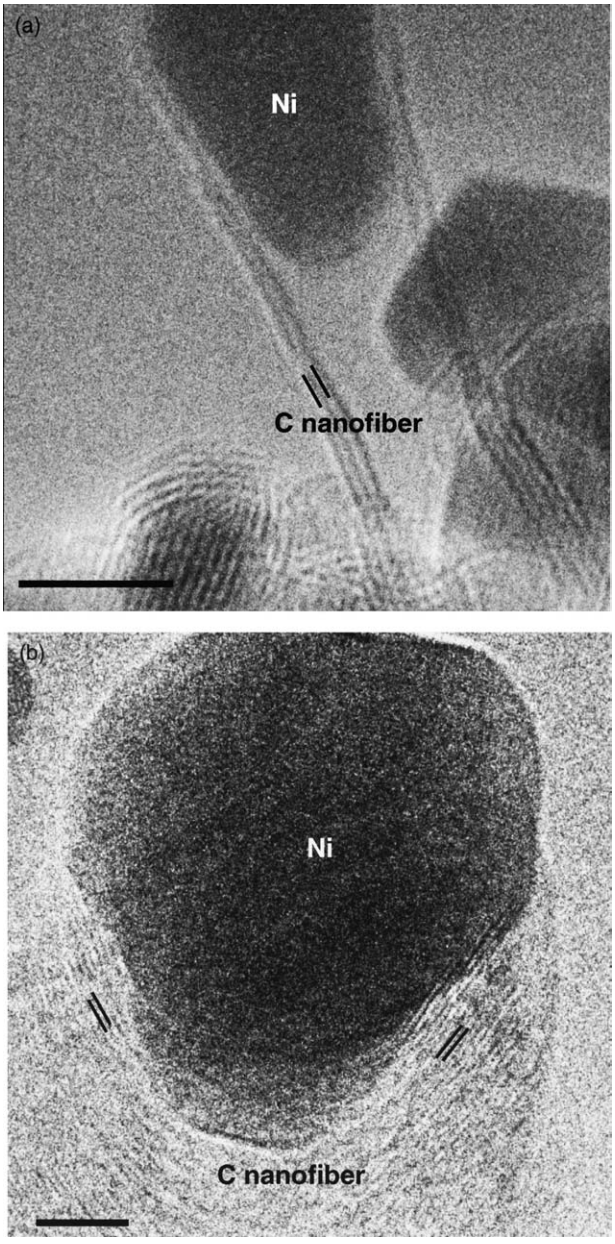

Fig. 3. HRTEM images of (a) a multi-walled tubular carbon nanofiber structure and (b) a whisker-type carbon nanofiber. The nanofibers are formed by exposing supported nickel nanocrystals to a mixture of CH_4:H_2 = 1:1 at a total pressure of about 2.0 mbar and a temperature of 500–540 °C. The lattice fringes in the nanofibers, indicated by the black lines, are separated by 0.34 nm, corresponding to the (0 0 2) lattice planes in graphite. Scale bar = 5 nm. Adapted from Ref. [16].

equilibrium shape of the Ni nanocrystal (∼6 nm in diameter) transforms into a highly elongated shape. The elongation of the Ni particle appears to be correlated with the formation of more graphene sheets at the graphene–Ni interface with their basal (0 0 2) planes oriented parallel to the Ni surface. Hence, the reshaping of the Ni nanocrystal assists the alignment of graphene layers into a tubular structure. The elongation of the Ni nanocrystal continues until it achieves an aspect ratio (length/width) of up to ∼4, before it abruptly contracts into a spherical shape within less than ∼0.5 s (Fig. 4H). This contraction is attributed to the fact that the increase in the Ni surface energy can no longer be compensated for by the energy gained when binding the graphitic fiber to the Ni surface. The elongation/contraction scenario continues in a periodic manner as the nanofiber grows. Furthermore, the growth stops if the graphene layers eventually encapsulate the Ni particle, indicating that part of the Ni surface must be in direct contact with the gas phase.

A closer inspection of the HRTEM movies reveals that mono-atomic steps are present at the Ni surface and play a key role in the nucleation and growth of graphene sheets. Ni step-edges are induced spontaneously in the course of the reaction, even at the graphene–Ni interface (Fig. 4B–G). An additional graphene layer appears in between the pair of such step-edges and the layer grows as the Ni steps move concurrently towards the ends of the Ni cluster and vanish. Clearly, this process involves transport of C atoms towards and Ni atoms away from the graphene–Ni interface. The flux of Ni atoms is directed towards the free Ni surface producing the observed elongation. Carbon atoms, resulting from methane decomposition at the free surface, must diffuse to the interface to account for the growth of the graphene layer. Since the TEM images represent two-dimensional projections of the sample, the observations are indicative of graphene growth around the nanoparticles. The graphene layer appears to extend around the Ni nanoparticles in an asymmetric fashion, because the interfacial step-edge formation can be observed at either side of the nanocluster at different instants (Fig. 4B and E). With an increasing diameter of up to 20 nm, the in situ HRTEM movies reveal that the Ni nanoparticles gradually tend to become more stable and pear-shaped [42]. For all sizes of the Ni nanoparticles, the movies reveal an interfacial growth scenario similar to that shown in Fig. 4, i.e. the step-edge assisted graphene growth is a general mechanism for the nickel-catalyzed growth of graphitic nanofiber structures under the present growth conditions.

The atomic-level observations can be rationalized through interplay with density functional theory (DFT) calculations. The DFT calculations show that methane dissociation is facilitated at step-edges and that carbon atoms bind stronger to step-edges than to facet sites [43]. This suggests that the step-sites act as the preferential nucleation sites for graphene. The extra binding energy of carbon to a step-site is in fact larger than the energy cost for step formation, which explains why steps form spontaneously at the Ni surface [16,43]. Moreover, the DFT calculations show that carbon atoms are more stable in a graphene layer than at a step-site showing that there is an energetic driving force for graphene growth. In the continuous growth of the multi-walled graphitic nanofibers, the graphene layers nucleate and grow preferentially at the existing graphene–Ni interface. This is suggested to be driven by an additional energy gain associated by binding a new graphene layer to the graphite matrix.

Furthermore, the observed surface dynamics can consistently be explained by a novel interfacial transport mechanism (Fig. 5). The experiments clearly point to the necessity of transport of Ni atoms towards the front of the Ni particles. The Ni atoms must diffuse along the nickel surface, because the Ni nanoparticles remain crystalline during growth (Fig. 6) and Ni

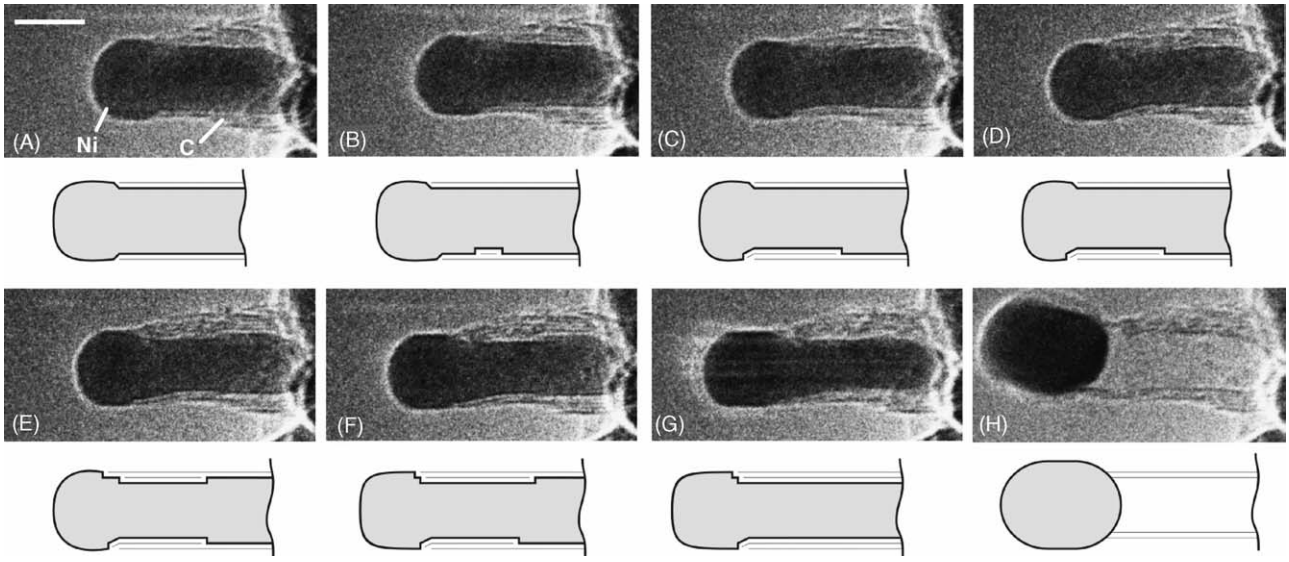

Fig. 4. In situ HRTEM image sequence of a growing carbon nanofiber (movies can be found in Ref. [42]). Images (A–H) illustrate one cycle in the elongation/contraction process. Drawings are included to guide the eye in locating the positions of mono-atomic Ni step-edges at the graphene–Ni interface. The images are acquired in situ with CH_4:H_2 = 1:1 at a total pressure of 2.1 mbar with the sample heated to 536 °C. All images are obtained with a rate of 2 frames/s. Scale bar = 5 nm. Adapted from Ref. [16].

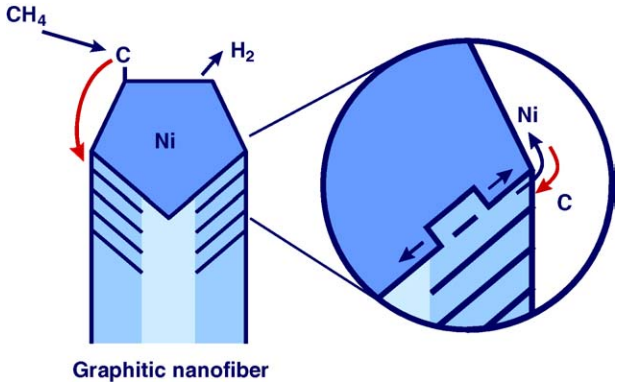

Fig. 5. Illustration of the growth mechanism for graphitic nanofibers formed by methane decomposition over nickel nanocrystals. The illustration highlights the surface transport of carbon and nickel atoms and the spontaneous Ni step-edge formation at the graphene–Ni interface.

diffusion through the bulk nickel nanocrystal cannot take place [44]. In accordance with this, the DFT calculations show that the Ni atomic transport can proceed as Ni surface diffusion along the free Ni surface and the graphene–Ni interface. Previously, it was suggested that transport of carbon atoms may proceed through the nickel bulk [35,39,45–47]. Although such an effect may occur under some growth conditions, the results in Ref. [16] suggest that it is not necessary to include bulk diffusion to obtain a consistent growth mechanism. The DFT calculations show that it is possible for C to migrate along the graphene–Ni interface and that a surface transport mechanism similar to that for nickel can also account for the transport of C atoms from the free surface of the Ni particle to sites at the graphene–nickel interface. The maximum activation energy barrier is associated with the carbon transport along the Ni surface and is estimated from the DFT calculations to be 1.6 eV.

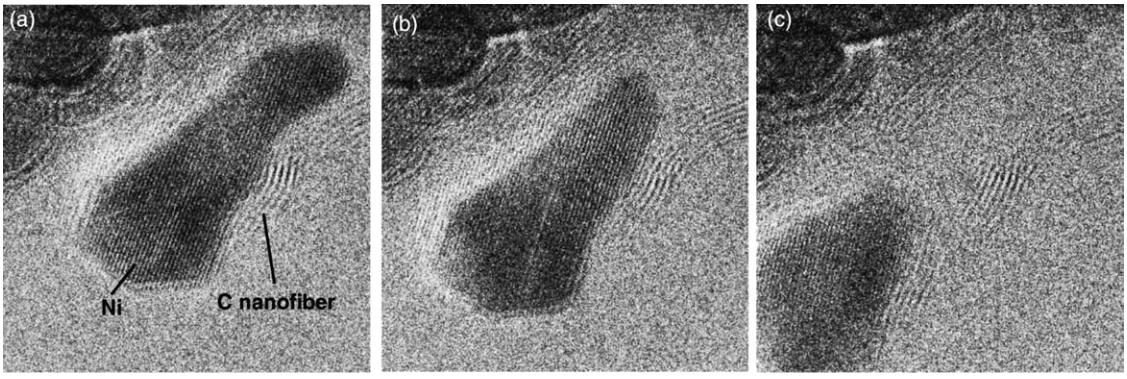

Fig. 6. Snapshots obtained from an in situ HRTEM movie of carbon nanofiber growth. The lattice-resolved images of the contracting Ni nanocrystal are obtained only when it is oriented with a zone-axis close to the electron beam. Several such image sequences show that the Ni nanocluster remain crystalline during the whole growth scenario. In the Ni nanocrystal, the lattice spacing is 0.20 nm corresponding to (1 1 1) planes in metallic Ni. In the carbon nanofiber, the lattice spacing is 0.33 nm corresponding to the (0 0 2) planes in graphite. The growth conditions: CH_4:H_2 = 1:1 at a total pressure of 2.1 mbar with the sample heated to 530 °C. The images are recorded at relative times (a) 0 s, (b) 2 s and (c) 5 s.

This is in reasonable agreement with the measured activation barrier for carbon nanofiber growth in the range 1.3–1.5 eV [35,45], suggesting that transport of carbon atoms confined to the nickel surface could be the rate-limiting step for nanofiber growth.

The in situ HRTEM observations and DFT calculations demonstrate that step-sites play an important role as growth centers for graphene growth, mainly because carbon binds more strongly to step-sites than to sites at the closed-packed facets on Ni. The preference of C atoms for step-site adsorption is found in general [48], and the mechanism may therefore be of general importance in metal-catalyzed growth of carbon nanofibers. Furthermore, the findings support the general understanding of the effect of many different promoters in Ni-based steam reforming catalysts: potassium, sulfur and gold promoter atoms were found to bind preferentially to Ni step-edges, suggesting that these elements suppress graphite formation through a step-blocking mechanism [38,43]. Recently, step site blocking was also demonstrated to provide control over the bond-breaking selectivity of higher hydrocarbons at nickel surfaces [49].

4. Concluding remarks

The examples highlighted here show that in situ HRTEM is now capable of providing atomic-scale insight into the structure and dynamics of supported metal nanoclusters. The finding that the nanoclusters can undergo dynamic shape changes in response to changes in the gas environment has the general implication that the distribution of catalytic active sites, and hence the catalytic activity, is self-regulated by the reaction conditions. Furthermore, it is discussed how information about the exposed metal surfaces and their gas-induced dynamic behavior can be combined with fundamental information about gas–surface interactions and how this can be included into the description of the catalytic properties of nanoclusters; this is often referred to as the materials and pressure gaps in catalysis. In this respect, it should be noted that in situ HRTEM investigations are presently carried out with rather modest pressures. Important future developments of in situ HRTEM are foreseen to introduce in situ cells, operating at higher pressures of up to, e.g., 1 bar, and on-line activity measurements that allow the detailed coupling between the active surfaces and their catalytic properties to be scrutinized at the atomic level.

Acknowledgements

The authors gratefully acknowledge J.B. Wagner, C. López-Cartes, J. Sehested, A.M. Molenbroek, H. Topsøe, B.S. Clausen, J.R. Rostrup-Nielsen, F. Abild-Pedersen and J.K. Nørskov for their contributions to the research included in the this article. The FEI Company is thanked for a fruitful collaboration on the development of the in situ HRTEM facility at Haldor Topsøe A/S, and the CTCI Foundation, Taiwan, is acknowledged for their financial participation.

References

[1] A.K. Datye, in: G. Ertl, H. Knözinger, J. Weitkamp (Eds.), Handbook of Heterogeneous Catalysis, vol. 2, Wiley–VCH, New York, 1997, pp. 493–512.
[2] J.M. Thomas, P.L. Gai, Adv. Catal. 48 (2004) 174.
[3] A. Bell, Science 299 (2003) 1688.
[4] H. Topsøe, J. Catal. 216 (2003) 155.
[5] D.A. Jefferson, P.J.F. Harris, Nature 332 (1988) 617.
[6] R.M. Stockman, et al., J. Mol. Catal. A Chem. 102 (1995) 147.
[7] J. Urban, H. Sack-Kongehl, K. Weiss, Catal. Lett. 49 (1997) 101.
[8] A.K. Datye, J. Catal. 216 (2003) 144.
[9] R.T. Baker, Catal. Rev. Sci. Eng. 19 (1979) 161.
[10] R.T. Baker, P.S. Harris, J. Phys. E Sci. Instrum. 5 (8) (1970) 793.
[11] E.D. Boyes, P.L. Gai, Ultramicroscopy 67 (1997) 219.
[12] R. Sharma, Microsc. Microanal. 7 (2001) 494.
[13] S. Sao-Joao, S. Giorgio, S. Nietche, C.R. Henry, in: Proceedings of 13th European Microscopy Congress, vol. II, 2004, p. 101.
[14] P.L. Hansen, et al., Science 295 (2002) 2053.
[15] J.B. Wagner, et al., J. Phys. Chem. B 107 (2003) 7753.
[16] S. Helveg, et al., Nature 427 (2004) 426.
[17] P.L. Hansen, S. Helveg, A.K. Datye, Adv. Catal., in press.
[18] J.A. Dumesic, H. Topsøe, Adv. Catal. 26 (1977) 121.
[19] B.S. Clausen, et al., Top. Catal. 1 (1994) 367.
[20] J.D. Grunwaldt, et al., J. Catal. 194 (2000) 452.
[21] B.S. Clausen, H. Topsøe, R. Frahm, Adv. Catal. 42 (1998) 315.
[22] J.W. Niemantsverdriet, Spectroscopy in Catalysis, Wiley–VCH, Weinheim, 2000.
[23] B.M. Weckhuysen, In-Situ Spectroscopy of Catalysts, American Scientific Publishers, California, 2004.
[24] C.V. Ovesen, et al., J. Catal. 168 (1997) 133.
[25] N.-Y. Topsøe, H. Topsøe, J. Mol. Catal. A Chem. 141 (1999) 95.
[26] J.B. Hansen, in: G. Ertl, H. Knözinger, J. Weitkamp (Eds.), Handbook of Heterogeneous Catalysis, vol. 4, Wiley–VCH, New York, 1997, pp. 1856–1876.
[27] C.T. Campbell, Surf. Sci. Rep. 27 (1997) 1.
[28] C.R. Henry, Surf. Sci. Rep. 31 (1998) 231.
[29] K.H. Hansen, et al., Phys. Rev. Lett. 83 (1999) 4120.
[30] L.V. Koplitz, O. Dulub, U. Diebold, J. Phys. Chem. B 107 (2003) 10583.
[31] E.G. Derouane, et al., J. Catal. 69 (1981) 101.
[32] R.T.K. Baker, P.S. Harris, R.B. Thomas, Surf. Sci. 46 (1974) 311.
[33] P.A. Crozier, A.K. Datye, Stud. Surf. Sci. Catal. 130 (2000) 3119.
[34] R. Sharma, Z. Iqbal, Appl. Phys. Lett. 84 (6) (2004) 990.
[35] R.T.K. Baker, et al., J. Catal. 26 (1972) 51.
[36] R.T.K. Baker, et al., J. Catal. 30 (1973) 86.
[37] J. Sehested, Catal. Today, 2005 (this issue).
[38] J.R. Rostrup-Nielsen, J. Sehested, J.K. Nørskov, Adv. Catal. 47 (2002) 65.
[39] K.P. de Jong, J.W. Geus, Catal. Rev. Sci. Eng. 42 (4) (2000) 481.
[40] P.M. Ajayan, Chem. Rev. 99 (1999) 1787.
[41] M. Terrones, Int. Mat. Rev. 49 (2005) 325.
[42] Examples of In situ HRTEM movies of the carbon nanofiber growth from [16] can be found at http://www.haldortopsoe.com/site.nsf/pages/nanotechnology.
[43] H.S. Bengaard, et al., J. Catal. 209 (2002) 365.
[44] D.R. Askeland, The Science and Engineering of Materials, second ed., PWS-KENT, Boston, 1989 (Chapter 5).
[45] D.L. Trimm, Catal. Rev. Sci. Eng. 16 (1977) 155.
[46] I. Alstrup, J. Catal. 109 (1988) 241.
[47] J.R. Rostrup-Nielsen, D.L. Trimm, J. Catal. 48 (1977) 155.
[48] J.K. Nørskov, et al., J. Catal. 209 (2002) 275.
[49] R.T. Vang, et al., Nat. Mater. 4 (2005) 160.